

Abstract 115 Table 1 Monocyte subset numbers

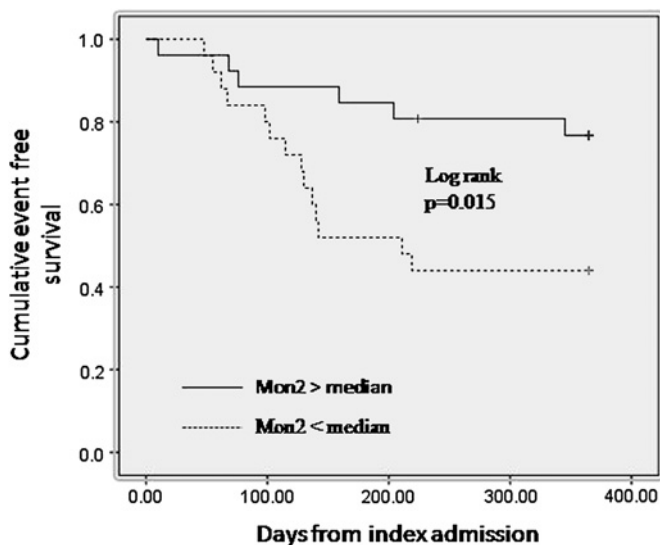
	AHF	SHF	CAD	HC	p Value
Total monocytes (per μ l)	852 \pm 300 ABC	646 \pm 172 D	541 \pm 139	502 \pm 190	<0.001
Mon1 (per μ l)	685 \pm 224 ABC	524 \pm 156 D	448 \pm 120	412 \pm 166	<0.001
Mon2 (per μ l)	59.9 (41.7–121) ABC	42.7 (30.0–68.7) DE	29.5 (15.3–46.6)	33.7 (10.1–52.9)	0.006
Mon3 (per μ l)	78.0 \pm 54.5 C	71.2 \pm 33.0	60.1 \pm 28.0	55.2 \pm 29.4	0.024

A= p <0.05 AHF vs SHF, B= p <0.05 AHF vs CAD, C= p <0.05 AHF vs HC, D= p <0.05 SHF vs HC, E= p <0.05 SHF vs CAD.

pathophysiology of heart failure (HF). We examined differences in monocyte subset numbers and expression of cell surface markers of activation (CD14) and chemotaxis (CCR2) in patients with acute HF (AHF), stable HF (SHF) and controls and evaluated their impact on clinical outcomes.

Methods Three monocyte subsets [CD14++CD16–CCR2+ (Mon1), CD14++CD16+CCR2+ (Mon2) and CD14+CD16++CCR2– (Mon3)] were analysed by flow cytometry in 51 patients with AHF, 42 patients with SHF, 44 patients with stable coronary artery disease (CAD) and 40 healthy controls (HC). Surface marker expression of CD14 and CCR2 was also measured and expressed as median fluorescent intensity (MFI). The prognostic impact of monocyte subsets was examined in patients with AHF.

Results Patients with AHF had significantly higher Mon1 counts compared to other groups (p <0.001 for all) (Abstract 115 table 1). Similarly, Mon2 counts were increased in AHF compared to SHF (p =0.011), CAD (p <0.001) and HC (p <0.001). Mon2 counts were also increased in SHF compared to both CAD and HC groups (p =0.023, p =0.035 respectively). In AHF, CD14 expression by Mon2 was significantly higher than in CAD patients (1481 \pm 473 vs 1228 \pm 408, p =0.039) and in SHF patients, CD14 expression by Mon2 was significantly higher than in CAD patients (1502 \pm 484 vs 1228 \pm 408, p =0.031). CCR2 expression by Mon2 in AHF was higher than in HC (128 \pm 43.9 vs 104 \pm 28.5, p =0.013) and CCR2 expression by Mon2 was higher in SHF compared to HC (126 \pm 36.2 vs



Abstract 115 Figure 1 Kaplan–Meier curves of cumulative event-free survival in patients with AHF for the primary end-point of mortality or re-hospitalisation. The groups are divided along the median value of Mon2 counts (59.9 cells/ μ l).

104 \pm 28.5, p =0.032). 20 patients (39.2%) with AHF reached the primary end point of death or re-hospitalisation, with a median time to event of 129 (IQR 70.0–209) days. In Cox regression analysis, after adjustment for age, left ventricular ejection fraction, serum creatinine and brain natriuretic peptide, Mon2 count remained an independent negative predictor of combined death and re-hospitalisation [HR (for an increase of 10 cells/ μ l) 0.829 (CI 0.713 to 0.964; p =0.015)]. In Kaplan–Meier analysis AHF patients with Mon2 above median (59.9 cells/ μ l) had significantly better outcomes compared to those below the median (Abstract 115 figure 1).

Conclusion We have shown for the first time that CD14++CD16+ monocytes (Mon2) are an independent negative predictor of adverse prognosis in patients with AHF. This subset is phenotypically different from the other monocyte subsets, with increased expression of markers of activation (CD14) and chemotaxis (CCR2). Consequently, the Mon2 subset merits further evaluation as a prognostic marker and potential therapeutic target in patients with HF.

116 MATRIX METALLOPROTEINASE INHIBITION ATTENUATES REPERFUSION INJURY, INDEPENDENTLY OF AND ADDITIVE TO MITOCHONDRIAL PERMEABILITY TRANSITION PORE INHIBITION

doi:10.1136/heartjnl-2012-301877b.116

¹R M Bell,* ¹Cara Hendy, ¹D Bruce-Hickman, ¹S Davidson, ²R Breckenridge, ¹D M Yellon. ¹Hatter Cardiovascular Institute, University College London, London, UK; ²MRC National Institute for Medical Research, London, UK

While matrix-metalloproteinase (MMP) inhibitors appear to protect against myocardial ischaemia/reperfusion injury, the mechanisms are poorly understood. We hypothesised that cardioprotection resultant from MMP inhibition is independent of mitochondrial permeability transition pore (mPTP), the end-effector of ischaemic postconditioning (iPOC). In ex-vivo and in-vivo mouse hearts, we investigated whether the MMP inhibitor, ilomostat (0.25 μ mol/l), at the onset of reperfusion, could engender protection in the absence of cyclophilin-D (CyPD), an initiator of mPTP opening, against injurious ischaemia/reperfusion. We have previously demonstrated that CyPD knockout (KO) hearts have inherent resistance to ischaemia/reperfusion injury, and cannot be further protected by either pre or post conditioning regimen. Therefore to further attenuate infarction in this model would require a mechanism independent of the mPTP. We found that ilomostat attenuated infarct size in wild type (WT) animals (37% \pm 2.8% to 22% \pm 4.3%, equivalent to ischaemic post conditioning (iPostC—6 cycles of 10sec reperfusion/ischaemia), 27% \pm 2.1%, p <0.05). CyPD KO hearts had smaller infarcts compared to their conditioned WT brethren (28% \pm 4.2%) and iPostC failed to protect, indicative of a pre-protected phenotype, yet ilomostat significantly attenuated infarct size in these hearts (11% \pm 3.0%, p <0.001). Moreover, the infarct size seen in the ilomostat treated KO hearts was significantly smaller than that seen in the ilomostat treated WT hearts (p <0.05), suggesting that mPTP and MMP inhibition is summative. Furthermore, ilomostat was found to be protective following prolonged injurious ischaemia (50 min), an injurious regimen that iPostC in WT was insufficient to protect against (49% \pm 7.8% to 31% \pm 2.8%, p <0.05). Interestingly, we found that delaying administration of ilomostat 15 min after the onset of reperfusion results in failure to protect the heart, indicating an effect upon early reperfusion injury, rather than post infarct remodelling. Isolated mouse WT myocytes, loaded with the potentiometric dye Tetramethyl Rhodamine Methyl Ester (TMRM) and exposed to laser light generate reactive oxygen species, a potent opener of the mPTP. The time to mPTP opening can therefore be used as an assay of drug interaction with the mPTP. Using cyclosporine as a positive control, we found that ilomostat, unlike cyclosporine, did not delay

mPTP and was equivalent to the vehicle negative control, indicating no interaction with mPTP in isolated cardiomyocytes. In conclusion, we demonstrate that cardioprotection by MMP inhibition is independent of CyPD/mPTP function and can augment the protection seen following iPostC even after prolonged cardiac ischaemia. We believe that this may be through a novel molecular target not implicated in the recognised preconditioning paradigm, and one that may have potential therapeutic implications for clinical practice through attenuating acute reperfusion injury in acute coronary syndromes.

117 CONDUCTION BLOCK INDUCED BY ACIDOSIS IN HL-1 MOUSE ATRIAL MYOCYTES CAN BE REVERSED BY ADMINISTERING THE GAP JUNCTIONAL COUPLER ROTIGAPTIDE

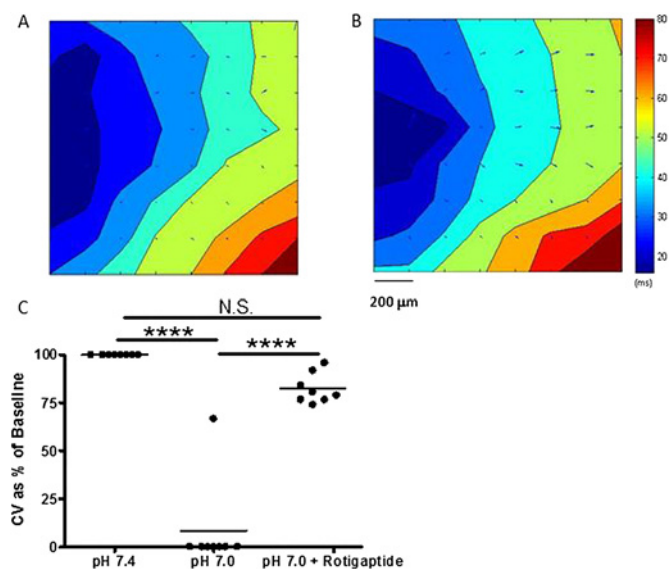
doi:10.1136/heartjnl-2012-301877b.117

S I Al-Aidarous,* C H Roney, F M D Peters, F S Ng, R A Chowdhury, N S Peters. Imperial College London, London, UK

Introduction Gap junctions (GJ) are low resistance intercellular pathways which play a major role in myocardial conduction and their remodelling is a key contributor to arrhythmogenic states. Rotigaptide has been shown to increase GJ coupling after ischaemic stress. However, the effect of rotigaptide in acidotic conditions is not well characterised. We hypothesised that rotigaptide can reverse GJ uncoupling and resultant decreases in conduction velocities (CV) brought about by a low pH in HL-1 mouse atrial myocytes.

Methods A subclone of HL-1 cells were seeded as a drop onto microelectrode arrays and were allowed to form a 2D monolayer. Baseline recordings were made at a physiological pH of 7.4 by pacing just above the intrinsic rate at a cycle length of 1000 ms for 10 s. The same preparations were subsequently incubated in media of pH 7.0 for 15 min. Incremental doses of 5 nM of rotigaptide were then added up to a maximum of 100 nM (n=8). Recordings were taken until no further changes in conduction velocities were seen.

Results A reduction of pH resulted in conduction block in all but one preparation (8.3%±23.6% of baseline, p<0.0001) and subse-



Abstract 117 Figure 1 (A) An activation map from stimulation at baseline pH 7.4. (B) An activation map from the same array after the cells had been subjected to a low pH then given rotigaptide. (C) Conduction velocities taken from microelectrode arrays at baseline, pH 7.0 and pH 7.0 + rotigaptide. ****p<0.0001.

quent addition of rotigaptide increased the CV (82.4%±7.8% of baseline, p<0.0001). The CV after addition of rotigaptide was not significantly different to that of the baseline (p>0.05). Activation maps were plotted and the direction of propagation was unchanged (p>0.05).

Conclusions Administration of rotigaptide resulted in the reversal of conduction block induced by acidosis without affecting the activation pattern in this atrial cell model. We suggest that acidosis in the absence of ischaemia is a sufficient insult to see an effect with rotigaptide. Therefore rotigaptide may be of use in the reversal of non-ischaemic conduction abnormalities. Further work is required to assess whether rotigaptide can also reverse conduction slowing in whole heart arrhythmogenic states.

118 FIRST PASS VASODILATOR-STRESS MYOCARDIAL PERFUSION CMR IN MICE ON A CLINICAL WHOLE-BODY 3 TESLA SCANNER: VALIDATION AGAINST MICROSPHERES

doi:10.1136/heartjnl-2012-301877b.118

R Jogiya,* M Makowski, A Phinikaridou, A Chiribiri, N Zarinabad, S Kozzerke, R Botnar, E Nagel, S Plein. Kings College London, London, UK

Background Animal models are important to develop our understanding of the pathophysiology of cardiovascular disease and for the development of new therapies. While coronary autoregulation maintains resting MBF constant over a wide range of pathological conditions, MBF reserve during hyperaemic stress is impaired in several common disease processes. First pass contrast-enhanced myocardial perfusion is the standard CMR method for the estimation of MBF and MBF reserve in man, but is challenging in rodents because of the constraints related to the high temporal and spatial resolution requirements.

Aim To evaluate first pass vasodilator stress myocardial perfusion CMR of the mouse heart against microspheres as the gold standard for regional organ flow.

Methods Five healthy 6-month old C57BL/6J mice were anaesthetized using 2% isoflurane. CMR imaging was performed on a clinical 3.0 Tesla scanner (Philips Healthcare, Best, the Netherlands) with a 23 mm single loop surface coil and a murine monitoring and ECG gating system (SA Instruments, NY, USA). Vasodilator stress was induced using a slow injection of dipyrimadole via a tail vein catheter. Stress perfusion data were acquired with an injection of gadolinium contrast (Gadobutrol 0.5 mmol/kg) 30 s later. The perfusion pulse sequence has been reported¹, in summary, it used a saturation recovery gradient echo method with 10-fold k-space and time domain undersampling with constrained image reconstruction using temporal basis sets (k-t PCA) to achieve a spatial resolution of 0.2×0.2×1.5 mm³ and an acquisition window of 43 ms. Following stress perfusion mice were recovered. One week later the mice underwent repeat anaesthesia and stress testing with LV injections of fluorescent microspheres at rest and at stress. Microsphere images were analysed using confocal microscopy.

Results Data were acquired successfully in all five mice. Mean heart rate increased from 480±27.4 bpm at rest to 503±41.5 bpm (p=0.08) during vasodilatation. Mean myocardial blood flow at rest by Fermi-function constrained deconvolution in control mice was 3.4±0.5 ml/g/min and increased to 8.9±3.0 ml/g/min during stress (ratio 2.6:1, p=0.036). The mean count of microspheres increased from rest to stress by a ratio of 2.7:1 (mean spheres per slice n=27±3.2, n=74±18.5, p=0.0005).

Conclusion First-pass myocardial stress perfusion CMR in a mouse model is feasible. Although the quantification of myocardial blood flow was lower than published values, the trend in myocardial blood flow was consistent with existing literature. Data were acquired on a 3 Tesla scanner using an approach similar to clinical acquisition